# IN-SITU RAMAN SPECTROSCOPY STUDIES OF OXYGEN SPILLOVER AT SOLID OXIDE FUEL CELL ANODES

G.M. Eliseeva<sup>1</sup>, I.N. Burmistrov<sup>1,2</sup>, D.A. Agarkov<sup>1,2</sup>, A.A. Gamova<sup>1</sup>, I.V. Ionov<sup>3</sup>,

M.N. Levin<sup>4</sup>, A.A. Solovyev<sup>3</sup>, I.I. Tartakovskii<sup>1,5</sup>, V.V. Kharton<sup>1</sup>, S.I. Bredikhin<sup>1,2</sup>

<sup>1</sup>Institute of Solid State Physics RAS, 142432, Russia, Moscow region, Chernogolovka, Academician Osipyan str., 2

<sup>2</sup>Moscow Institute of Physics and Technology, 141700, Russia, Moscow region, Dolgoprudniy, Institutskiy per., 9

<sup>3</sup>Institute of High Current Electronics, Siberian Branch RAS, 634055, Russia, Tomsk, Akademichesky Av., 2/3

<sup>4</sup>EFKO Group, Biruch Innovation Center, 309927, Russia, Belgorod region, Malobykovo <sup>5</sup>National Research University Higher School of Economics, 101000, Russian, Moscow, Myasnitskaya Str. 20, e-mail: agarkov@issp.ac.ru

**Abstract:** The present work is centered on the combined studies of anodic processes in electrode-supported solid oxide fuel cells (SOFCs) using in-situ Raman spectroscopic and electrochemical measurements. A possibility to perform direct spectroscopic measurements at the inner electrolyte | anode interface in the case of anode-supported SOFC with polycrystalline thin-film zirconia solid electrolyte was experimentally demonstrated. The application of anode-supported SOFC architecture makes also it possible to significantly extend the range of operating temperatures and current densities across the electrochemical cell. The results confirm a direct incorporation of oxygen anions transported through zirconia electrolyte into the ceria-based anode sublayer, with subsequent fuel oxidation at the cermet anode.

**Key words:** solid oxide fuel cell, in-situ Raman spectroscopy, anode-supported SOFC, optical transparency, inner interface.

### Introduction

Solid oxide fuel cells (SOFCs) transform chemical energy of hydrogen [1] and hydrocarbon fuels [2] into the electrical and heat energy [3]. The SOFC efficiency is higher compared to other power generation technologies [4], especially in the case of hybrid systems where SOFCs are combined with gas turbines [5]. The SOFC efficiency depends, however, on an electrode optimization level and degradation processes [6]. The in-situ spectroscopic analyses of SOFC components under operating conditions have a key importance for electrode optimization. In particular, one important challenge is to understand microscopic mechanisms of the anodic fuel oxidation in order to optimize anode architecture on the basis of direct experimental data. Conventional techniques of the structural and elemental analyses (e.g., scanning electron microscopy, SEM, energy-dispersive X-ray spectroscopy, EDX, X-ray diffraction, XRD, X-ray photoelectron spectroscopy, XPS) cannot be used for this goal due to severe working conditions of SOFCs, namely operating temperatures from 550 to 900°C [7], high current densities up to 3-4 A/cm<sup>2</sup> [8-9], chemically aggressive atmospheres, and separated gas chambers with fuel and oxidant mixtures. On the contrary, Raman spectroscopy provides possibilities for the *in-situ* studies of operating SOFCs [10-11]. Moreover, very large databases of Raman spectra exist in the literature for different types of chemical reactions and materials, including those used in SOFCs [12-13]. Attractive applications of Raman spectroscopy for the in-situ studies of operating solid oxide fuel cells include so-called "spectro-chronopotentiometry" (correlation of the electrochemical performance with spectral data) [14], monitoring of Ag-Cr interactions at the SOFC cathode [15], assessment of mechanical stresses [16-17], and surface mapping [18]. At the

same time, most literature data were only collected from the outer surfaces of electrodes or solid electrolytes due to the low penetration depth of light.

This work presents the results obtained on model SOFCs with a novel geometry, based on an optically transparent thin-film polycrystalline solid electrolyte membrane made of stabilized cubic zirconia. The membrane transparency in combination with ring-shaped cathode enables to pass the laser excitation beam across solid electrolyte and to collect scattered radiation from the inner "anode | electrolyte" interface, simultaneously measuring the current vs. voltage dependencies and impedance spectra of the electrochemical cell. Similar *in-situ* approach proposed in our previous works [19-23] was based on the use of zirconia single crystals as the membrane of electrolyte-supported cells (ESCs). However, the ESC geometry substantially limits the range of working temperatures and currents due to high ohmic resistance of the thick (~ 250 µm) zirconia membrane; its thickness also leads to the dominance of cubic zirconia contribution visible in the Raman spectra. In order to solve these problems, thin anode-supported zirconia films were magnetron-sputtered and tested in the present work.

# **Experimental methods and materials**

Cell fabrication and characterization

The geometry of model anode-supported cells with the thin-film electrolyte membrane of yttria-stabilized zirconia (YSZ) is illustrated in Fig.1.

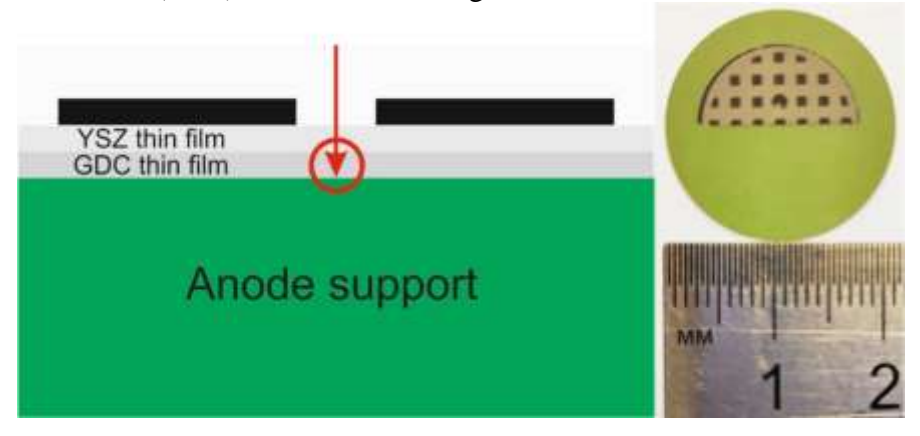


**Figure 1.** Architecture (left) and photograph (right) of anode-supported SOFCs developed in this work. Red arrow shows laser beam; black layer at the top of electrochemical cell corresponds to the ring-shaped cathode.

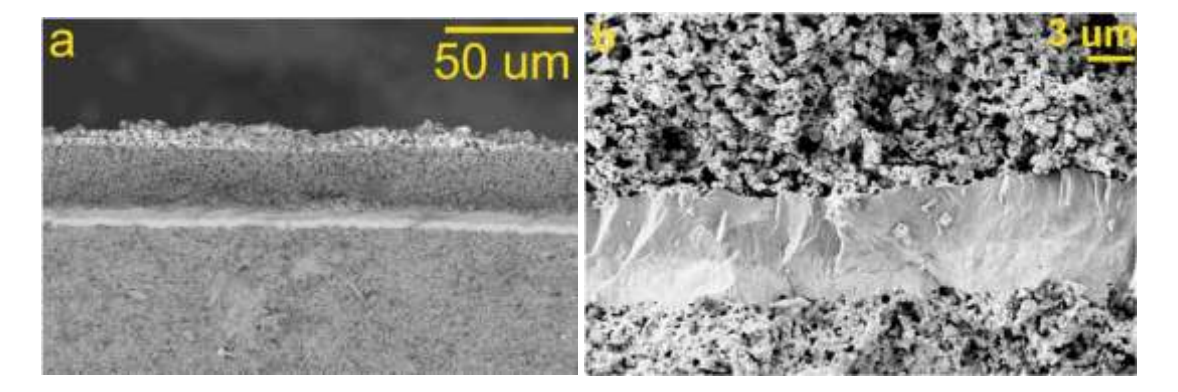


**Figure 2.** SEM images showing cross-sections of the model SOFCs with different magnifications. The cathode layer is at the top.

The commercial anode supports made of NiO-YSZ composite were supplied by SOFCMAN (China). Thin anode sublayers of 10 mol.% gadolinia-doped ceria (10GDC) were deposited onto the porous anode supports by magnetron sputtering at the Institute of High

Current Electronics SB RAS. In standard SOFCs, such sublayers are necessary to facilitate anodic reactions and to suppress carbon deposition due to high catalytic activity and mixed ionic-electronic conductivity of reduced ceria. In the case of Raman spectroscopy, these sublayers play an additional role, indicating local overpotential as their spectra lines exhibit a significant dependence on the oxygen nonstoichiometry of GDC; the related phenomena are discussed below. Then gas-tight membrane films of 8YSZ (92 mol% ZrO<sub>2</sub> + 8 mol% Y<sub>2</sub>O<sub>3</sub>) solid electrolyte with the thickness of 3-5 μm were magnetron-sputtered onto 10GDC sublayers. The deposition was performed using two 85/15 at.% Zr/Y targets (size of 300x100x6 mm<sup>3</sup>, distance from the anode support of 10 cm) in Ar-O<sub>2</sub> mixture at 300°C and operating total pressure of 0.3 Pa. Subsequent screen-printing of the ring-shaped cathodes made of lanthanum-strontium manganite (LSM), was similar to that in our previous reports [24-27]. Fig.2 presents two SEM micrographs illustrating high quality of the solid-electrolyte films and specific morphology of the electrode layers (LSM cathode is at the top, NiO-YSZ anode is at the bottom).

The optical transparency of polycrystalline 8YSZ films was studied using a Specord M40 spectrometer (Carl Zeiss Jena, Germany) in a wavelength range from 200 to 900 nm. These measurements were performed for the films with thicknesses of 1.6, 3.0 and 4.7  $\mu$ m, sputtered onto single-crystal 8YSZ supports (300  $\mu$ m). The magnetron sputtering conditions were identical to those used in the course of SOFC fabrication. As an illustration, Fig.3 displays cross-section of the sample with 4.7  $\mu$ m thickness, finally annealed at 1100°C.

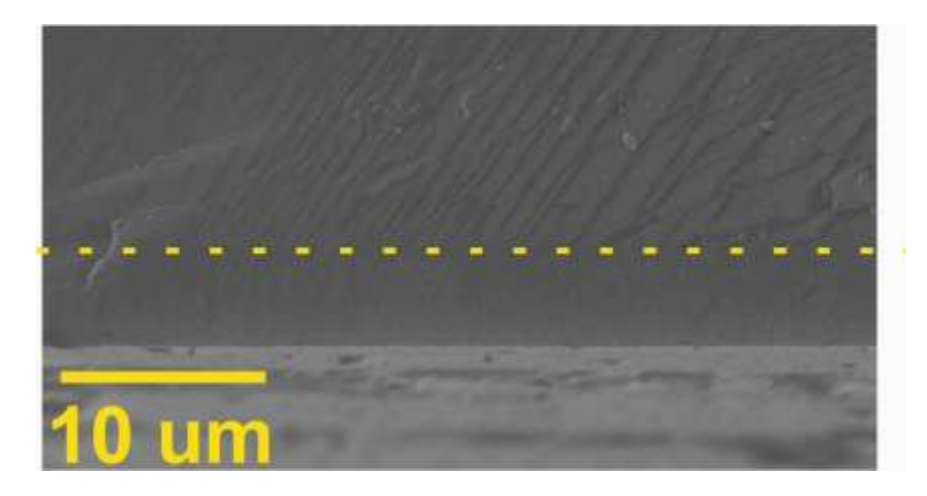


**Figure 3.** Cross-section of 8YSZ sample comprising a 4.7 μm thick film deposited onto single crystal of the same composition, for the optical transparency studies.

The microstructure of individual materials and electrochemical cells was characterized by scanning electron microscopy (SEM) using a LEO Supra 50VP and a Dual Beam VERSA 3D HighVac (FEI) instruments.

Electrochemical measurements were performed using Gamry Reference 3000 potentiostat/galvanostat/ZRA.

Setup for in-situ Raman studies and electrochemical measurements

The *in-situ* Raman studies of SOFC anodes were carried out using a combined experimental setup consisting of optical and electrochemical blocks. The main part of this setup, except for potentiostat and temperature controller connected to the measuring cell, is shown in Fig. 4.

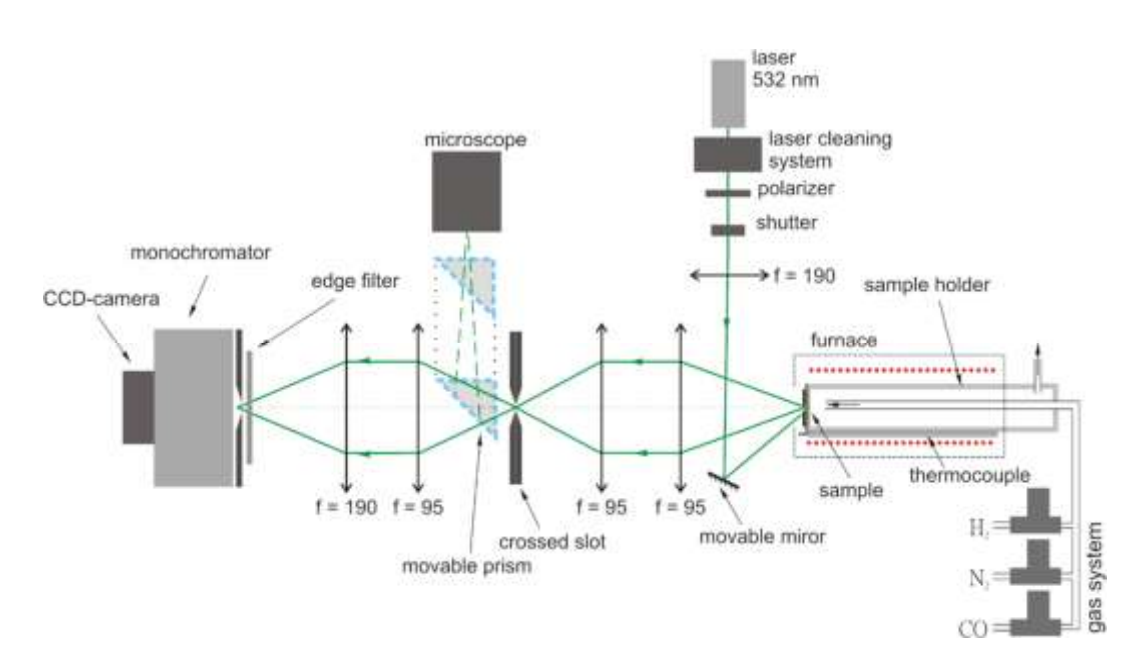


**Figure 4.** Principal scheme of the combined experimental setup for *in-situ* Raman studies and electrochemical measurements.

The high-temperature holder made of a single-crystal sapphire tube (produced by ISSP RAS) is fixed on a computer-controlled mechanical system (Avesta-Project, Russia) for precise placing of the sample; a button-type SOFC sample is sealed onto one end of this tube. The gas system comprising a set of mass-flow controllers (Bronkhorst, Netherlands) makes it possible to supply mixtures of H<sub>2</sub>, N<sub>2</sub> and CO into the anode chamber. The optical part of the setup consists of an excitation radiation sub-system and an optical sub-system for the scattered radiation detection. A multimode semiconductor green laser (wavelength of 532 nm; power output of 20 mW), with a 532 nm spectroscopic filter and a polarizer, was selected as a source of the excitation radiation. A mechanical iris-type shutter placed on the laser beam trajectory was used to collect background spectra for their subtraction from the final Raman spectra. All the lenses used for the setup were supplied by the Lytkarino Factory of Optical Glass (Russia). A movable prism-type mirror was used to direct scattered radiation to a microscope with a computer-controlled CCDcamera (ToupView, China) during tuning of the sample position. A pair of lenses (focus distances of 95 and 190 mm) directs the scattered radiation onto the edge filter and then onto a hole of a diffraction grating spectrometer (MDR-12, LOMO, Russia); finally the spectra were collected using a liquid nitrogen-cooled CCD-camera LN/CCD-1340/400-EHRB/1 produced by Roper Scientific (USA) with the size of 1340x400 pixels.

#### **Results and discussion**

The data on optical transparency of the polycrystalline 8YSZ films sputtered onto 300 µm-thick 8YSZ single crystals are summarized in Figure 5.

The black line corresponding to the single-crystal support is almost constant, close to 75% in the studied wavelength range. The deposition of polycrystalline thin films leads to a progressive decrease in the transmittance at large wavenumbers. As expected, this effect associated with extended defects in the polycrystalline films becomes more pronounced when the film thickness increases. Nonetheless, the films remain optically-transparent in the wavelength range used for the Raman studies, marked by black rectangle in Fig.5. and should not noticeably affect collected Raman spectra. One should also mention that the transmittance of polycrystalline films exhibits periodic dependence on the wavenumbers due to light interference. The average period of these dependences can be used to estimate refractive index, varying from  $(2.4\pm0.2)$  for the film thickness of 4.7  $\mu$ m up to  $(2.5\pm0.2)$  for 1.6  $\mu$ m. Such values well correspond to the refractive indexes of stabilized zirconia [28-30].

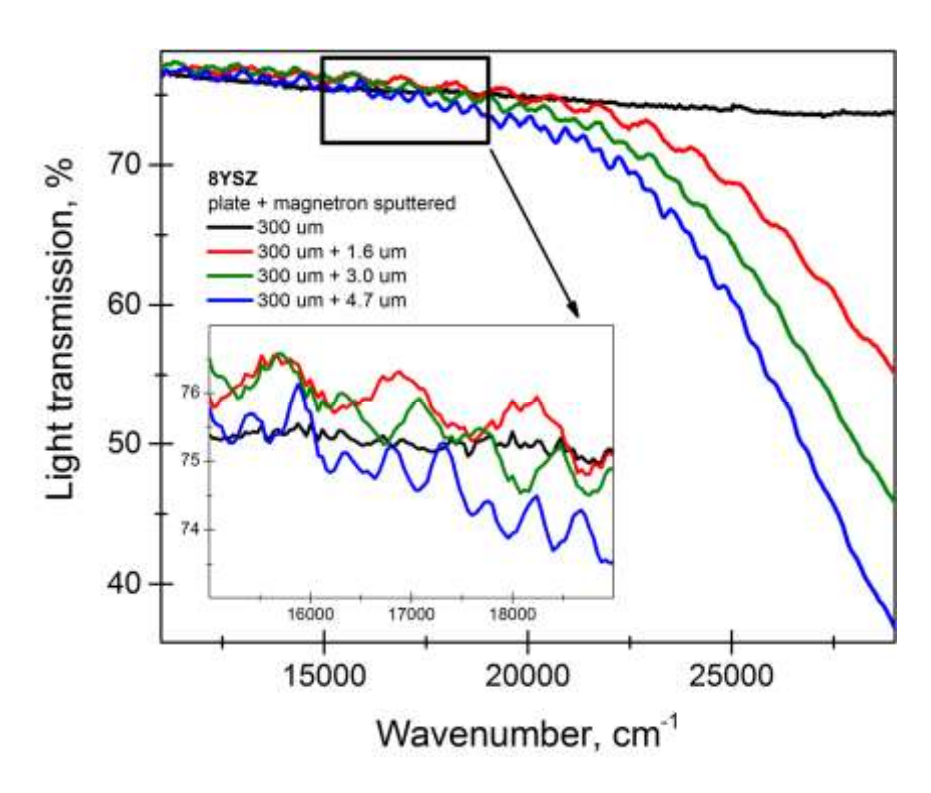


**Figure 5.** Transmittance spectra of magnetron-sputtered 8YSZ layers compared to that of 8YSZ single-crystal support. The film thicknesses are given in the legend.

Figures 6 and 7 illustrate electrochemical performance of the model anode-supported SOFC with thin-film 8YSZ membrane supported by cermet anode.

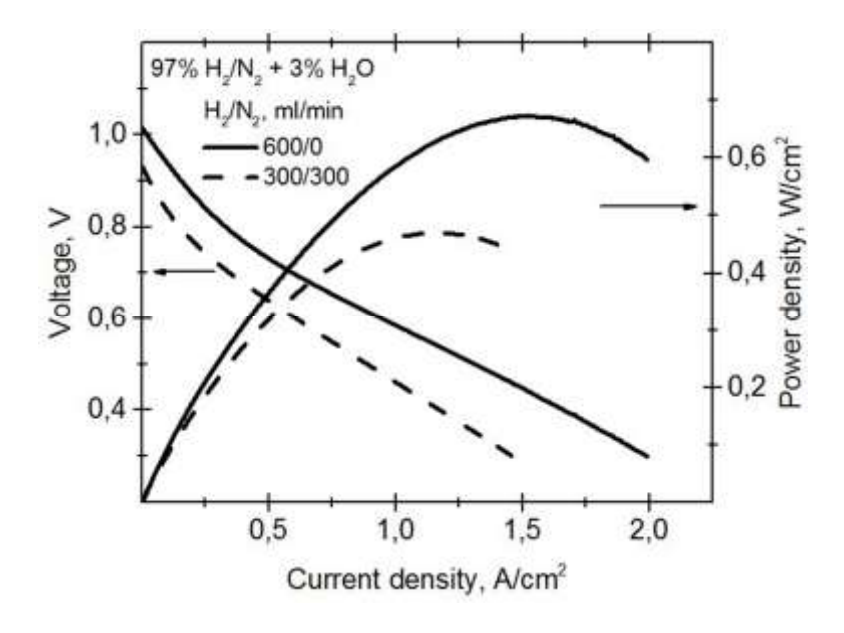


**Figure 6.** Voltage and power vs. current density dependencies of the model SOFCs for two different fuel mixture compositions (vol.%): 97%  $H_2 - 3\%$   $H_2O$  and 48.5%  $H_2 - 48.5\%$   $N_2 - 3\%$   $H_2O$ . The total fuel mixture flow rate was 600 ml/min.

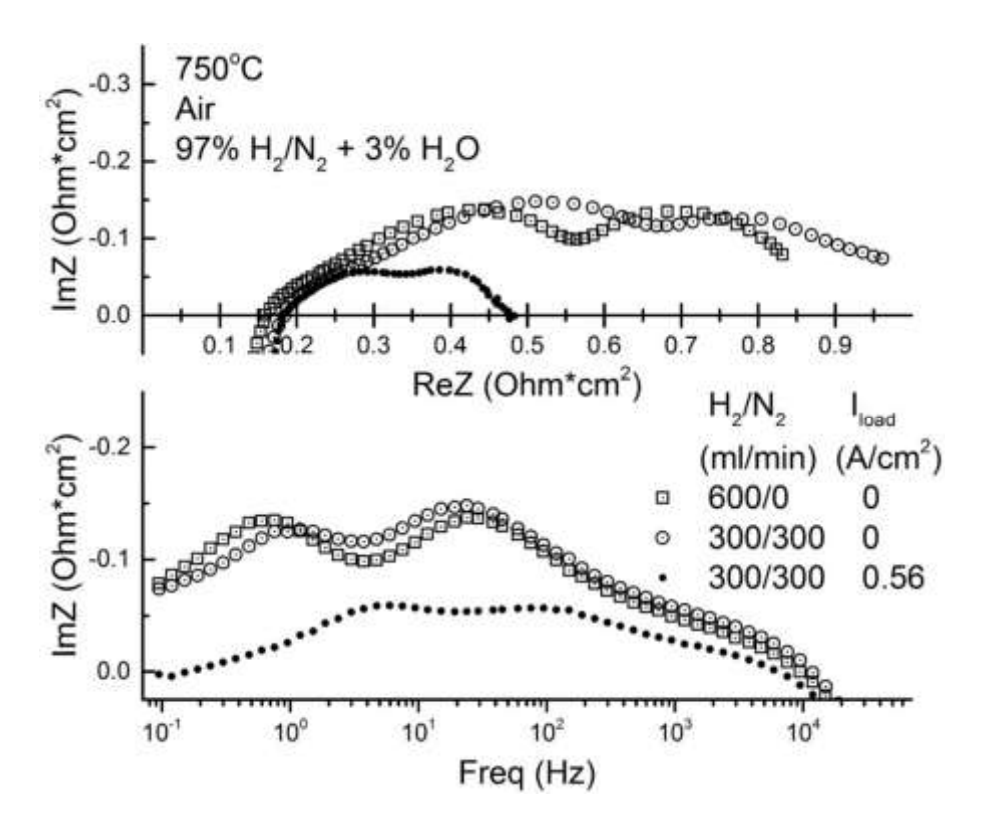


**Figure 7.** Impedance spectra of the model anode-supported SOFC for two different fuel mixture compositions (vol.%): 97%  $H_2 - 3\%$   $H_2O$  and 48.5%  $H_2 - 48.5\%$   $N_2 - 3\%$   $H_2O$ , under open circuit conditions ( $I_{load} = 0$ ) and at the current density of 0.56 A/cm<sup>2</sup>. The total fuel mixture flow rate was 600 ml/min.

The open circuit voltage (OCV) for humidified hydrogen is higher than 1 V, which gives a direct evidence of satisfactory gas-tightness of the solid electrolyte membrane and sealing. The maximum power density is higher than  $0.6 \text{ W/cm}^2$ , acceptable for practical applications. The ohmic resistance of the cell is lower than  $0.2 \text{ Ohm} \times \text{cm}^2$ . Decreasing hydrogen pressure leads to a modest decrease of low-frequency  $(10^{-1}\text{-}1 \text{ Hz})$  contribution in the impedance spectra, Fig.7; the intermediate-frequency contribution observed at  $10^1\text{-}10^2 \text{ Hz}$  tends to slightly increase, probably due to partial surface oxidation of nickel in the cermet anode. Note that the low-frequency arc diminishes at high current densities.

Raman spectra collected from the inner GDC  $\mid$  electrolyte interface of the anode-supported SOFC at room temperature and at  $750^{\circ}\text{C}$  are presented in Figures 8a and 8b, respectively.

One can observe several overlapped peaks associated with zirconium and cerium oxides. The most intensive of them is attributed to ceria; zirconia signals are much lower compared to the electrolyte-supported cells [21,23]. The NiO peaks could also be separated from the room-temperature spectrum of oxidized anode, but their intensity is too low. Furthermore, due to relatively high operating temperature of SOFCs, the intensity of thermal radiation becomes excessive. In order to improve the measurement statistics, cyclic accumulation of the signal was used and the subtraction of the heated body radiation spectrum was performed for each cycle. One example of the resultant spectrum is shown in Figure 8b. Such spectra were then normalized to the temperature-frequency factor (Fig.8c) and used for deconvolution by Gaussian lines (Fig.8d). The latter procedure was necessary in order to suppress the errors associated with partial overlapping with the zirconia peaks. The deconvolution makes it possible to separate the Ce-O-Ce peak (~460 cm<sup>-1</sup>) sensitive to the local oxygen stoichiometry.

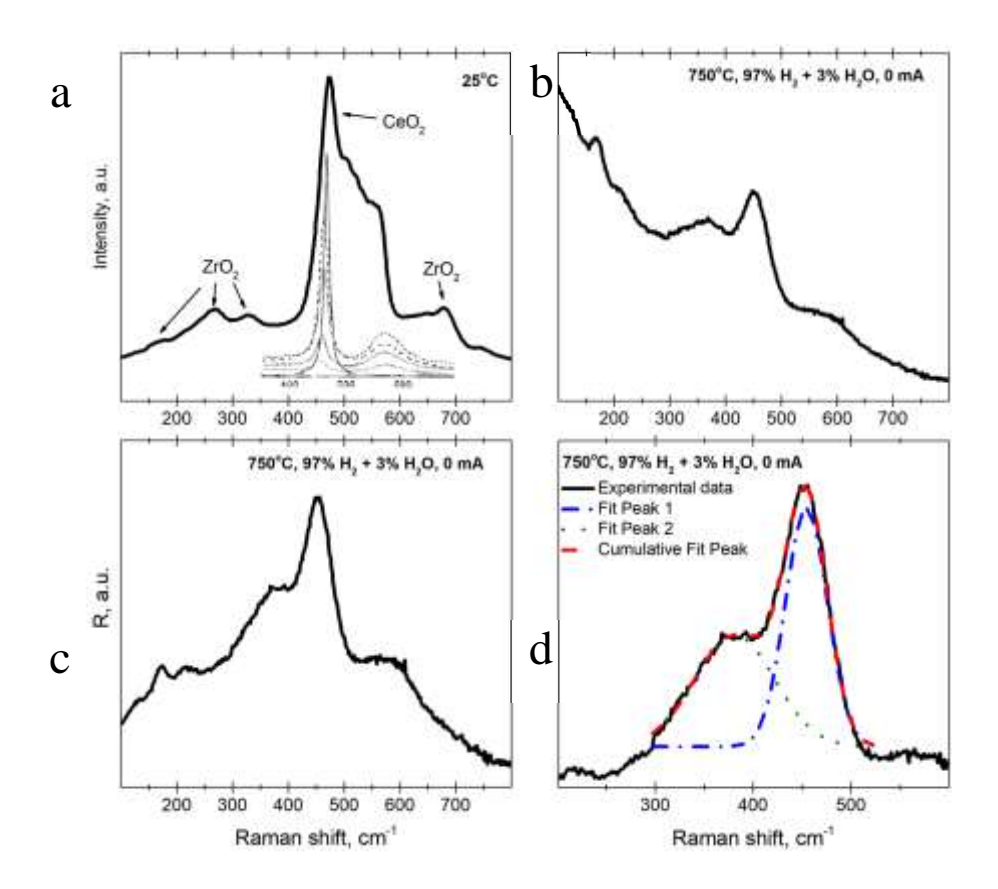


**Figure 8.** Raman spectra from the inner "anode | electrolyte" interface at room temperature (a) and at 750°C (b). The inset in (a) displays characteristic peak with the shift of 460 cm<sup>-1</sup> in the spectra of doped ceria, which is extremely sensitive to oxygen stoichiometry variations [31-32]. The high-temperature Raman spectrum was collected for 100 measuring cycles (1 second each). The parts (c) and (d) show the high-temperature spectrum normalized to the temperature-frequency factor and deconvolution of this spectrum by Gaussian lines, respectively.

The dependences of the extracted ~460 cm<sup>-1</sup> peak intensity on fuel mixture composition and current load are displayed in Fig.9.

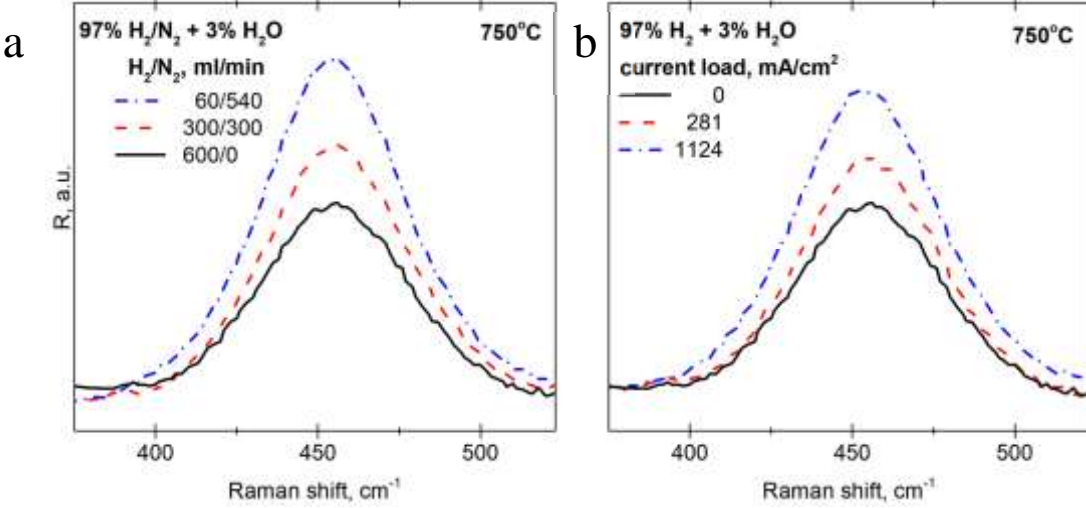


**Figure 9.** Intensity of the Ce-O-Ce spectral line vs. fuel gas mixture composition (a) and current (b).

As expected, the intensity of the Ce-O-Ce peak is strongly dependent on the electrochemical potential of oxygen at the anode, determining oxygen nonstoichiometry of

doped ceria at a fixed temperature. Namely, this signal becomes higher when the content of oxygen in the crystal lattice increases as photons scatter more frequently on the phonons corresponding to symmetric oscillations of Ce cations between oxygen anions. As a result, the peak intensity decreases with increasing hydrogen partial pressure and increases with increasing anodic current density. This behavior is similar to that observed for the electrolyte-supported SOFCs with ceria-containing anodes [23]. It indicates a direct incorporation of oxygen anions transported across zirconia membrane into the GDC lattice with subsequent fuel oxidation, confirming the so-called oxygen spillover mechanism of the anodic process.

#### **Conclusions**

The combined studies of electrode processes in the anode-supported solid oxide fuel cells using *in-situ* Raman spectroscopic and electrochemical measurements, were performed. The possibility of direct spectroscopic measurements at the inner electrolyte | anode interface in the case of polycrystalline thin-film zirconia solid electrolyte was experimentally demonstrated by the optical transparency tests and Raman investigations. The use of anode-supported SOFC architecture makes also it possible to significantly extend the range of operating temperatures and current densities compared to the electrolyte-supported cells. The results confirm that oxygen anions are directly transported from YSZ electrolyte membrane into the ceria-based anode sublayer, providing an evidence in favor of the oxygen spillover mechanism.

# Acknowledgements

This study was financially supported by Russian Scientific Foundation, grant 17-79-30071 "Scientifically grounded optimization of power and mass-dimensional characteristics of planar SOFC stacks and development of fuel processor for highly-efficient transport and stationary power plants". Study was supported by the Ministry of Science and Higher Education of Russian Federation, unique identifier of contract RFMEFI60819X0279 "Development of stacks of anode-supported solid oxide fuel cells for highly-efficient generator of hydrogen energy" in the part of development of model anode-supported SOFC fabrication technology.

## References

- 1. Bessler W.G., Warnatz J., Goodwin D.G. The influence of equilibrium potential on the hydrogen oxidation kinetics of SOFC anodes. *Solid State Ionics*. 2007, vol. 177, iss. 39-40, pp. 3371-3383.
- 2. Gorte R.J., Vohs J.M. Novel SOFC anodes for the direct electrochemical oxidation of hydrocarbons. *J. Catal.* 2003, vol. 216, iss. 1-2, pp. 477-486.
- 3. Stambouli A.B., Traversa E. Solid oxide fuel cells (SOFCs): a review of an environmentally clean and efficient source of energy. *Renew. Sust. Energ. Rev.* 2002, vol. 6, iss. 5, pp. 433-455.
- 4. Raymond R.A. Status of tubular SOFC field unit demonstrations. *J. Power Sources*. 2000, vol. 86, iss. 1-2, pp. 134-139.
- 5. Akkaya A.V., Sahin B., Erdem H.H. An analysis of SOFC/GT CHP system based on exergetic performance criteria. *Int. J. Hydrog. Energy.* 2008, vol. 33, iss. 10, pp. 2566-2577
- 6. Ding D., Li X., Lai S.Y., Gerdes K., Liu M., Enhancing SOFC cathode performance by surface modification through infiltration. *Energ. Environment. Sci.* 2014, iss. 7, pp. 552-575.
- 7. Charpentier P., Fragnaud P., Schleich D.M., Gehain E. Preparation of thin film SOFCs working at reduced temperature. *Solid State Ionics*. 2000, vol. 135, iss. 1-4, pp. 373-380.
- 8. Solovyev A.A., Rabotkin S.V., Shipilova A.V., Ionov I.V. Magnetron sputtering of gadolinium-doped ceria electrolyte for intermediate temperature solid oxide fuel cells. *Int. J. Electrochem. Sci.* 2019, vol. 14, pp. 575-584.

- 9. Smolyanskiy E.A., Linnik S.A., Ionov I.V., Shipilova A.V., Semenov V.A., Lauk A.L., Solovyev A.A. Magnetron sputtered LSC thin films for solid oxide fuel cell application. *J. Phys.: Conf. Ser.* 2018, vol. 1115, pp. 032080.
- 10. Cheng Z., Liu M. Characterization of sulfur poisoning of Ni–YSZ anodes for solid oxide fuel cells using *in-situ* Raman microspectroscopy. *Solid State Ionics*. 2007, vol. 178, iss. 13-14, pp. 925-935.
- 11. Pomfret M.B., Marda J., Jackson G.S., Eichhorn B.W., Dean A.M., Walker R.A. Hydrocarbon fuels in solid oxide fuel cells: in situ Raman studies of graphite formation and oxidation. *J. Phys. Chem. C.* 2008, vol. 112, iss. 13, pp. 5232-5240.
- 12. Lee J.-W., Liu Z.. Yang L., Abernathy H., Choi S.-H., Kim H.-E., Liu M. Preparation of dense and uniform La<sub>0.6</sub>Sr<sub>0.4</sub>Co<sub>0.2</sub>Fe<sub>0.8</sub>O<sub>3-δ</sub> (LSCF) films for fundamental studies of SOFC cathodes. *J. Power Sources*. 2009, vol. 190, iss. 2, pp. 307-310.
- 13. Cheng Z., Abernathy H., Liu M. Raman Spectroscopy of Nickel Sulfide Ni3S2. *J. Phys. Chem. C.* 2007, vol. 111, iss. 49, pp. 17997-18000.
- 14. Kirtley J.D., Halat D.M., McIntyre M.D., Eigenbrodt B.C., Walker R.A. High-temperature "spectrochronopotentiometry": correlating electrochemical performance with in situ Raman spectroscopy in solid oxide fuel cells. *Anal. Chem.* 2012, vol. 84, iss. 22, pp. 9745-9753.
- 15. Abernathy H.W., Koep E., Compson C., Cheng Z. Liu M. Monitoring Ag-Cr Interactions in SOFC Cathodes Using Raman Spectroscopy. *J. Phys. Chem. C.* 2008, vol. 112, iss. 34, pp. 13299-13303.
- 16. Nagai M., Iguchi F., Onodera S., Sata N., Kawada T., Yugami H. Evaluation of stress conditions in operated anode supported type cells based on *in-situ* Raman scattering spectroscopy. *ECS Trans.* 2011, vol. 35, iss. 1, pp. 519-525.
- 17. Van herle J., Ihringer R., Sammes N.M., Tompsett G., Kendall K., Yamada K., Wen C., Kawada T., Ihara M., Mizusak J. Concept and technology of SOFC for electric vehicles. *Solid State Ionics*. 2000, vol. 132, pp. 333-342.
- 18. Eigenbrodt B.C., Walker R.A. High temperature mapping of surface electrolyte oxideconcentration in solid oxide fuel cells with vibrational Raman spectroscopy. *Anal. Methods.* 2011, vol. 3, pp. 1478-1484.
- 19. Agarkov D.A., Burmistrov I.N., Tsybrov F.M., Tartakovskii I.I., Kharton V.V., Bredikhin S.I., Kveder V.V. Analysis of interfacial processes at the SOFC electrodes by *in-situ* Raman spectroscopy. *ECS Trans.* 2015, vol. 68, iss. 1, pp. 2093-2103.
- 20. Agarkov D.A., Burmistrov I.N., Tsybrov F.M., Tartakovskii I.I., Kharton V.V., Bredikhin S.I. Kinetics of NiO reduction and morphological changes in composite anodes of solid oxide fuel cells: estimate using Raman scattering technique. *Russ. J. Electrochem.* 2016, vol. 52, no. 7, pp. 600-605.
- 21. Agarkov D.A., Burmistrov I.N., Tsybrov F.M., Tartakovskii I.I., Kharton V.V., Bredikhin S.I. *In-situ* Raman spectroscopy analysis of the interfaces between Ni-based SOFC anodes and stabilized zirconia electrolyte. *Solid State Ionics*. 2017, vol. 302, pp. 133-137.
- 22. Bredikhin S.I., Agarkov D.A., Aronin A.S., Burmistrov I.N., Matveev D.V., Kharton V.V. Ion transfer in Ni-containing composite anodes of solid oxide fuel cells: a microstructural study. *Mater. Lett.* 2018, vol. 216, p. 193-195.
- 23. Agarkov D.A., Burmistrov I.N., Tsybrov F.M., Tartakovskii I.I., Kharton V.V., Bredikhin S.I. *In-situ* Raman spectroscopy analysis of the interface between ceriacontaining SOFC anode and stabilized zirconia electrolyte. *Solid State Ionics*. 2018, vol. 319C, pp. 125-129.
- 24. Burmistrov I., Agarkov D., Bredikhin S., Nepochatov Yu., Tiunova O., Zadorozhnaya O. Multilayered electrolyte-supported SOFC based on NEVZ-Ceramics membrane. *ECS Trans.* 2013, vol. 57, iss. 1, 917-923.

- 25. Burmistrov I.N., Agarkov D.A., Tsybrov F.M., Bredikhin S.I. Preparation of membraneelectrode assemblies of solid oxide fuel cells by co-sintering of electrodes. *Russ. J. Electrochem.* 2016, vol. 52, no. 7, pp. 669-677.
- 26. Burmistrov I.N., Agarkov D.A., Korovkin E.V., Yalovenko D.V., Bredikhin S.I. Fabrication of membrane-electrode assemblies for solid oxide fuel cells by joint sintering of electrodes at high temperature. *Russ. J. Electrochem.* 2017, vol. 53, no. 8, pp. 873-879.
- 27. Burmistrov I.N., Agarkov D.A., Tartakovskii I.I., Kharton V.V., Bredikhin S.I. Performance optimization of cermet SOFC anodes: an evaluation of nanostructured Ni. *ECS Trans.* 2015, vol. 68, iss. 1, pp. 1265-1274.
- 28. Briois P., Lapostolle F., Demange V., Djurado E., Billard A. Structural investigations D.A. Agarkov, et al. Solid State Ionics 344 (2020) 115091 8 of YSZ coatings prepared by DC magnetron sputtering. *Surf. Coat. Technol.* 2007, vol. 201, pp. 6012–6018,
- 29. Xiao Q., Hongbo H., Shao S., Shao J., Fan Z. Influences of deposition rate and oxygen partial pressure on residual stress and microstructure of YSZ thin films. *Thin Solid Films*. 2009, vol. 517, pp. 4295–4298.
- 30. Heiroth S., Ghisleni R., Lippert T., Michler J., Wokaun A. Optical and mechanical properties of amorphous and crystalline yttria-stabilized zirconia thin films prepared by pulsed laser deposition. *Acta Mater.* 2011, vol. 59, pp. 2330–2340.
- 31. McBride J.R., Hass K.C., Poindexter B.D., Weber W.H. Raman and X-ray studies of Ce<sub>1-x</sub>RE<sub>x</sub>O<sub>2-y</sub>, where RE=La, Pr, Nd, Eu, Gd and Tb. *J. Appl. Phys.* 1995, vol. 76, pp. 2435-2441.
- 32. Weber W.H., Haas K.C., McBride J.R. Raman study of CeO<sub>2</sub>: second-order scattering, lattice dynamics, and particle-size effects. *Phys. Rev. B.* 1993, vol. 48, n. 1, pp. 178-185.

# IN-SITU ИССЛЕДОВАНИЯ ТРАНСПОРТА КИСЛОРОДА В АНОДАХ ТВЕРДООКСИДНЫХ ТОПЛИВНЫХ ЭЛЕМЕНТОВ МЕТОДОМ СПЕКТРОСКОПИИ КОМБИНАЦИОННОГО РАССЕЯНИЯ СВЕТА

Г.М. Елисеева $^{1}$ , И.Н. Бурмистров $^{1,2}$ , Д.А. Агарков $^{1,2}$ , А.А. Гамова $^{1}$ , И.В. Ионов $^{3}$ , М.Н. Левин $^{4}$ , А.А. Соловьев $^{3}$ , И.И. Тартаковский $^{1,5}$ , В.В. Хартон $^{1}$ , С.И. Бредихин $^{1,2}$ 

<sup>1</sup>Федеральное государственное бюджетное учреждение науки Институт физики твердого тела Российской академии наук (ИФТТ РАН), 142432, Россия, Московская обл., г. Черноголовка, ул. Академика Осипьяна, д. 2

<sup>2</sup>Федеральное государственное автономное образовательное учреждение высшего образования «Московский физико-технический институт (национальный исследовательский университет)» (МФТИ), 141700, Россия, Московская обл., г. Долгопрудный, Институтский пер., д. 9

<sup>3</sup>Федеральное государственное бюджетное учреждение науки Институт сильноточной электроники Сибирского отделения Российской академии наук (ИСЭ СО РАН), 634055, Россия, г. Томск, Академический пр-кт, д. 2/3

<sup>4</sup>ГК ЭФКО, Инновационный центр Бирюч, 309927, Россия, Белогородская обл., с. Малобыково

<sup>5</sup>Федеральное государственное автономное образовательное учреждение высшего образования «Национальный исследовательский университет «Высшая школа экономики» (НИУ ВШЭ), 101000, Россия, г. Москва, ул. Мясницкая, д. 20 e-mail: agarkov@issp.ac.ru

Данная работа сфокусирована на комбинированных исследованиях анодных процессов в твердооксидных топливных элементах (ТОТЭ) с поддерживающим электродом методом *in-situ* спектроскопии комбинационного рассеяния света и при Экспериментально показана возможность помощи электрохимических измерений. проведения прямых спектроскопических исследований с внутреннего интерфейса электролит | анод в случае ТОТЭ с поддерживающей анодной подложкой и твердым электролитом на базе тонкопленочного поликристаллического стабилизированного диоксида циркония. Применение архитектуры ТОТЭ с поддерживающим анодом также дало возможность существенно расширить диапазон рабочих температур и плотности электрохимическую ячейку. Полученные токовых нагрузок через подтверждают прямое встраивание анионов кислорода, транспортируемых через циркониевый электролит в анодный подслой на базе диоксида церия, с последующим окислением топлива на керметном аноде.

**Ключевые слова:** твердооксидный топливный элемент, *in-situ* спектроскопия комбинационного рассеяния света, ТОТЭ с поддерживающим анодом, оптическая прозрачность, внутренний интерфейс.